

ARE THE SPECTRAL SHIFTS AN OPERATIONAL CONCEPT ?

CRITICAL ANALYSIS OF THEORETICAL AND EXPERIMENTAL RESULTS

F. BARET, S. JACQUEMOUD,* C. LEPRIEUR, G. GUYOT

INRA Bioclimatologie, BP91, 84143 Montfavet cedex, France

** LERTS, 18 Avenue E. Belin, 31400 Toulouse, France*

INTRODUCTION

With the recent development of imaging spectrometers, increasing attention has been paid to the interpretation of the new kind of information which can be obtained. Several studies have been carried out at differing scales, from the leaf to the canopy seen from space, in order to extract the vegetation biophysical characteristics from the monitored reflectance spectra. Most of the studies are focussed on the red edge, between 650 and 800 nm. This spectral domain corresponds to a sharp variation of the vegetation optical properties. A large number of studies report some spectral shifts termed blue shifts when shifting towards shorter wavelengths or red shifts when shifting towards longer wavelengths. These shifts are characterized by the wavelength of a particular point of the red edge. Authors generally refer to the inflection point the wavelength of which is termed λ_i . At leaf level, and mainly through experimental observations, λ_i is related to the chlorophyll concentrations and leaf structure (Gates, 1965; Horler *et al.*, 1983, Guyot *et al.*, 1990). The same trends are observed at canopy level, but with large scattering due to the effect of canopy geometry and external parameters such as the irradiance conditions and the viewing geometry (Collins, 1978; Chang and Collins, 1983; Collins *et al.*, 1983; Ferns *et al.*, 1984; Miller *et al.*, 1985; Gauthier and Neville, 1985; Baret *et al.*, 1987; Rock *et al.*, 1988a, 1988b; Demetriades-Shah and Steven, 1988). If all of these authors usually conclude that spectral shifts are of interest to characterize vegetation status, none has tried to rigorously demonstrate the additional information contained in the criteria derived from high spectral resolution. Furthermore, they generally agree on the complex nature of this spectral deformation, but few works explicitly quantify the λ_i sensitivity to canopy characteristics or external factors (Guyot *et al.*, 1990). The aim of this paper is to discuss the interest of λ_i in comparison with information content and signification of the classical single broad bands or vegetation indices. Finally, we will try to give an overview of the problems linked to a spatial determination of λ_i in terms of noise level and radiometric resolution capabilities. The discussion will be mainly carried out from theoretical data obtained through model simulations, but also with real AVIRIS data for the spatialization.

1. Equivalence between λ_i and single-band reflectance at leaf level

We have used the radiative transfer model elaborated by Jacquemoud and Baret (1990) to study the sensitivity of λ_i to leaf characteristics. This model requires only 2 input variables to compute, with a good accuracy, the leaf reflectance and transmittance

in the red edge domain : the Chlorophyll a and b concentration (C_{ab}) and an index related to the mesophyll structure (N). For compact leaves, N is close to one. For very thick and spongy mesophyll, N increases up to 2. It requires also three spectrally dependent parameters : the refractive index ($n(\lambda)$), the absorption coefficient of a compact leaf layer deprived of pigments and water ($k_o(\lambda)$), and the specific absorption coefficient of chlorophyll a and b ($K_{ab}(\lambda)$). $n(\lambda)$ which slowly and regularly decreases from 400 to 2500 nm has been set to its mean value ($n=1.442$). The $k_o(\lambda)$ absorption coefficient is approximated by :

$$k_o(\lambda) = 0.0114 - 4.87 \cdot 10^{-6} \cdot \lambda \quad [1]$$

$K_{ab}(\lambda)$ is described by a generalized logistic fit in the red edge. The sharp variation of K_{ab} , as seen on figure 1, is the cause of the red edge.

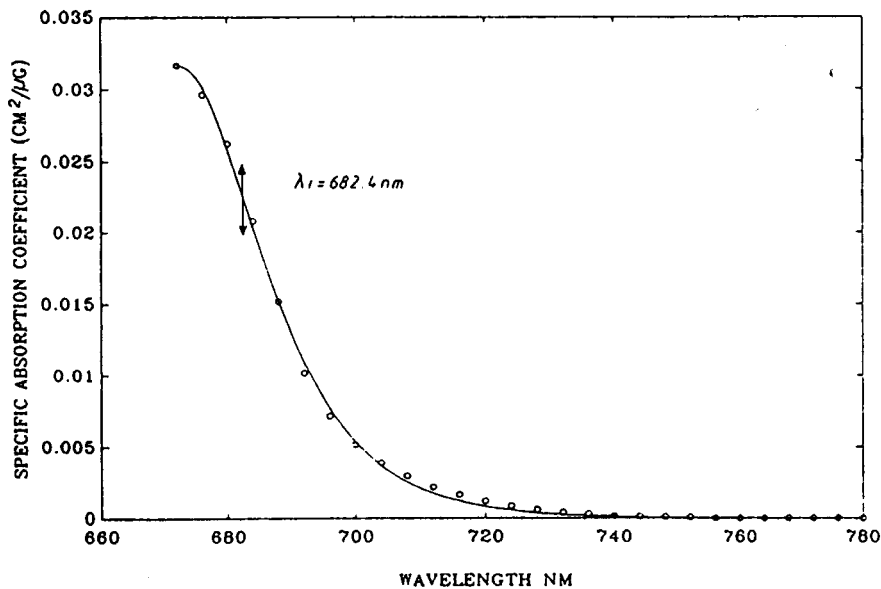


Figure 1. Specific absorption coefficient of chlorophyll a and b spectrum (from Jacquemoud and Baret, 1990). The solid line corresponds to a generalized logistic fit used in the formal derivation.

As an important remark, one can notice the dissymmetry of the specific absorption coefficient K_{ab} which probably induces a dissymmetry of the red edge. k_i is computed by formal derivation of this analytical model. Figures 2a and 2b demonstrate that λ_i mainly depends on chlorophyll concentration but also on the mesophyll structure parameter N which is in good agreement with previous results (Horler *et al.*, 1983). An increase in the chlorophyll concentration C_{ab} as well as an increase in the mesophyll structure parameter N produces a red shift. The transmittance is more sensitive to the structure parameter than the reflectance. λ_i varies from 683 nm for albino leaves deprived of pigments, to a maximum value close to 715 nm for a thick dark green leaf with a spongy mesophyll.

The question is now to demonstrate if this spectral deformation criterion provides any new information as compared with classical broad wavebands. We have plotted in a 3D space λ_i as a function of red (672 nm) and near infrared (780 nm) reflectance (respectively ρ_{672} and ρ_{780}) for a large range of variation of C_{ab} (from 1 to 70 g.cm⁻² with 1 g.cm⁻² step) and N (from 1.0 to 2.5 with 0.1 step). Figure 3 shows that the resulting surface is very smooth.

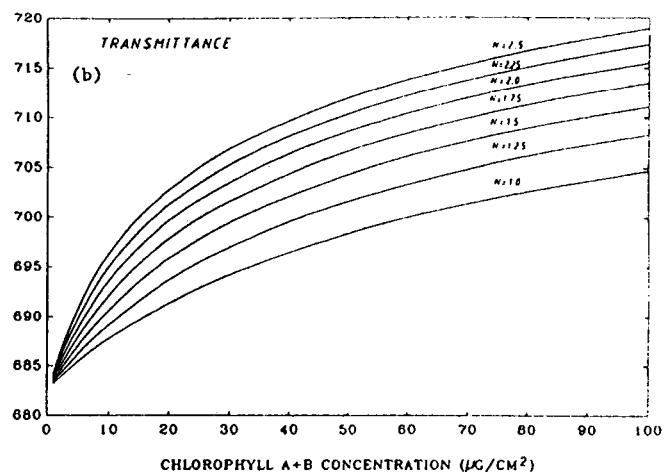
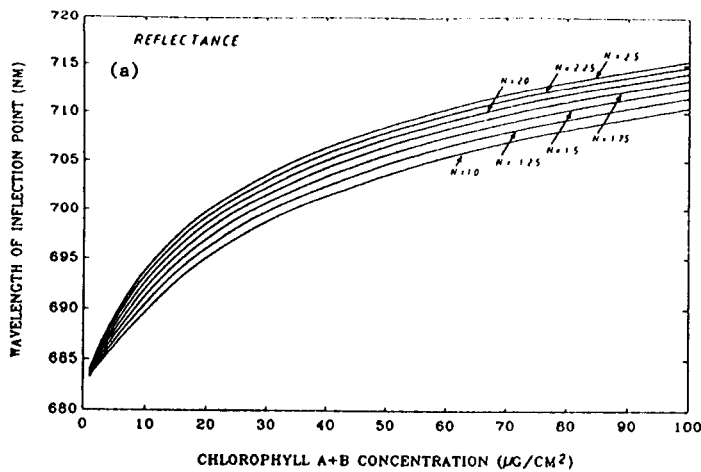


Figure 2. Effects of chlorophyll concentrations and mesophyll structure (represented by the N parameter) on reflectance (a) and transmittance (b) inflection point λ_i . Results from Jacquemoud and Baret (1990) model simulations.

It has been fitted to a 4th order polynomial surface and leads to a very low root mean square (rms=0.73 nm). It can be concluded that, at leaf level, the spectral shifts observed in the red edge are equivalent to the combined red and near infrared wavebands :

$$\lambda_i = f(\rho_{672}, \rho_{780}) [2]$$

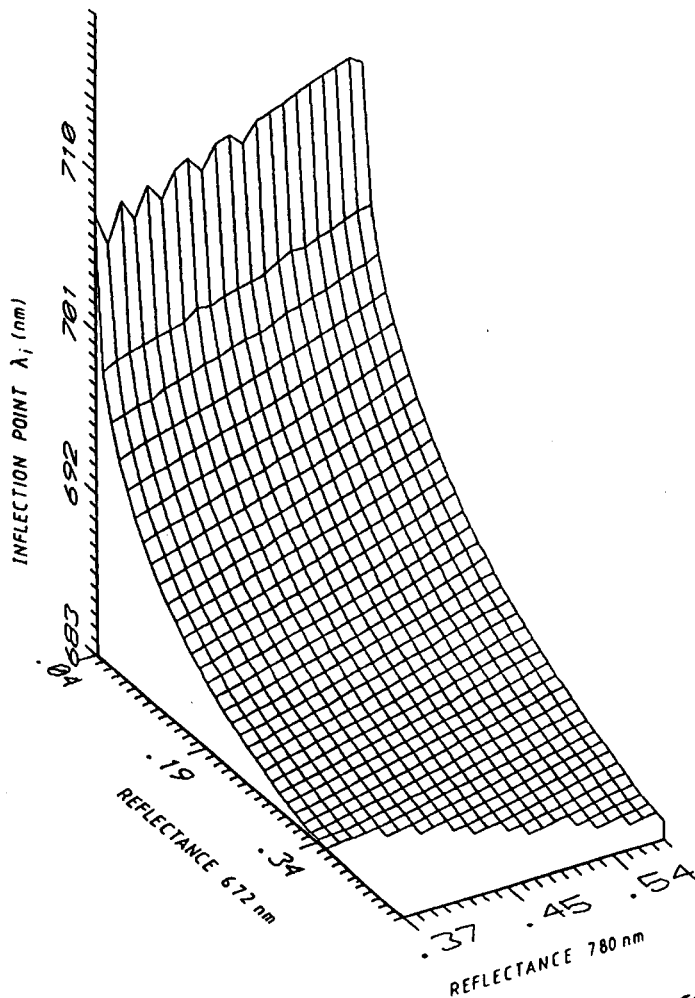


Figure 3. 3D representation of the function f relating λ_i to ρ_{672} and ρ_{780} .

This important property can be easily explained by the fact that λ_i is a function of C_{ab} and N , ρ_{780} depends on N and ρ_{672} is also determined by both N and C_{ab} :

$$\lambda_i = g(C_{ab}, N) ; \rho_{780} = h(N) ; \rho_{672} = i(C_{ab}, N)$$

$$\lambda_i = g(i^{-1}(\rho_{672}, h^{-1}(\rho_{780})), h^{-1}(\rho_{780})) = f(\rho_{672}, \rho_{780}) \quad [3]$$

Figure 2 reveals that λ_i is sensitive to changes in C_{ab} levels even for high values of C_{ab} as compared to the sensitivity of ρ_{672} which is close to the saturation level for C_{ab} close to 30 g.cm⁻² (Jacquemoud and Baret, 1990). But there is no difficulty to choose a particular wavelength in the red edge with a better sensitivity for higher C_{ab} values. Because no inflection point can be experimentally measured on spectra with a minimum of 3 data points, the determination of λ_i is no more of interest at leaf level. In the following section, we shall discuss the properties of λ_i at canopy level.

2. The nature of spectral shifts observed on canopies.

2.1. Method of λ_i computation.

To simulate canopy reflectance spectra and analyse the factors governing λ_i , we shall couple the preceding model of leaf optical properties with the SAIL (Verhoef, 1984, 1985) canopy reflectance model. This approach provides an analytical formulation of the canopy spectral reflectance ($R(\lambda)$) in the simple case of a one layer canopy with 90% directional incident radiation and 10% diffuse isotropic radiation irrespectively to the wavelength :

$$R(\lambda) = R(n(\lambda), k_o(\lambda), K_{ab}(\lambda), C_{ab}, N, LAI, \theta_o, \psi_o, \theta_s, \theta_1, \rho_s(\lambda)) \quad [4]$$

where LAI is the leaf area index, θ_o and ψ_o respectively the view zenith and azimuth angles, θ_s the solar zenith angle, θ_1 the mean leaf inclination angle characterizing the leaf angle distribution function (in this case we have used ellipsoidal distributions : Campbell, 1986; Wang and Jarvis, 1986), ρ_s the soil background reflectance. In equation (4), only four terms are spectrally dependent. The first 3 are the spectral parameters of the leaf model described in the previous section. The last one, $\rho_s(\lambda)$ is assumed to be linearly wavelength dependent and verifies the soil line concept (Richardson and Wiegand, 1977) with mean values of soil line parameters (Guyot and Baret, 1990) :

$$\rho_s(780) = 1.2.\rho_s(672) + 0.04 \quad [5]$$

This leads to the following equation relating ρ_s to λ and $\rho_s(672)$ taken as a soil brightness variable :

$$\rho_s(\lambda) = \rho_s(672) + ((\lambda-672)/(780-672)).(0.2.\rho_s(672)+0.04) \quad [6]$$

The canopy spectral reflectance can then be set in the form of a function of the wavelength and a convenient notation vector of input variables which are not wavelength dependent :

$$R(\lambda) = F(\lambda, X) \text{ with } X = (C_{ab}, N, LAI, \theta_o, \psi_o, \theta_s, \theta_1, \rho_s(672)) \quad [7]$$

Henceforth, analytical derivation of F is possible. Because of the complexity of the second derivative expression which is required to compute λ_i , we have defined the implicit function $F^2(\lambda, X)$ as :

$$F^2(\lambda, X) = d^2F/d\lambda^2 \quad [8]$$

It can be mathematically demonstrated that, assuming the continuity of F^2 , and the existence and continuity of $d(F^2)/d\lambda$, the solution λ_i that equates F^2 to zero, exists and is unique. The λ_i solution is then numerically computed for each values of X input variables vector. We are now able to analyse the sensitivity of λ_i to the X values.

2.2. sensitivity analysis.

We will restrict the study to vertical viewing ($\theta_0 = 0$). Because the LAI is one of the main factors controlling the biophysical processes at canopy level, we shall analyse, at each step, the interaction between the LAI and any other input variable. The simulations show that the main factors governing the shifts are the chlorophyll concentration and, to a lesser extent, the leaf area index. Any increase of C_{ab} or LAI produces a red shift (figure 4a). This is in good agreement with experimental results obtained on chlorotic plants where the decrease in C_{ab} is generally linked to a decrease of the LAI (Demetriades-Shah and Steven, 1988; Rock *et al.*, 1988b). For LAI greater than 4, the amplitude of the shift when C_{ab} increases from 1 to 80 $g.cm^{-2}$ is not very different from that observed on leaf reflectance spectra (about 40 nm). For a green crop, let say C_{ab} greater than 40 $g.cm^{-2}$, the λ_i range of variation with LAI is reduced to 15 nm. But this amplitude of variation is reduced again when the canopies are more planophile (figure 4c). This effect of canopy geometry agrees with experimental results of Vanderbilt *et al.* (1988), even in the absence of simulated specular effects. The leaf mesophyll structure produces also red shifts (figure 4b) : in comparison with a compact monocotyledonous leaf ($N=1.0$), a dicotyledonous thick and spongy mesophyll leaf ($N=2.0$) shifts λ_i towards longer wavelength of about 5 nm which is not negligible if one reminds the 15 nm amplitude observed for green vegetation. Soil brightness (figure 4d) affects only slightly λ_i for intermediate LAI. Further simulations reveal the insignificant influence of irradiance conditions (sun position and diffuse/direct incoming radiation ratio) on λ_i .

From this sensitivity analysis, we have come to the conclusion that λ_i was mainly influenced by canopy parameters, particularly by the chlorophyll a and b concentration and the leaf area index. External or disturbing factors, such as soil brightness or irradiance conditions, have only little effects on λ_i . This criterion can also be of interest for high spectral resolution studies. We have to notice the small amplitude of variation which may restrict its efficiency in case of measurements performed with a relatively low accuracy. But we have still to discuss about the redundancy level with classical single wavebands.

2.3. Comparison with classical single wavebands or vegetation indices.

For a given wavelength, equation (7) states that the same set of input parameters (X vector) governs single reflectance band. As previously seen at leaf level, we will then test if the information provided by λ_i is equivalent to that contained in classical bands or in vegetation indices. We have simulated ρ_{672} , ρ_{780} , and λ_i for a large range of X vectors. The practical problem lies in the great number of arrangements if one wants to cross all of them. Hence, the input variables have been chosen at random according to

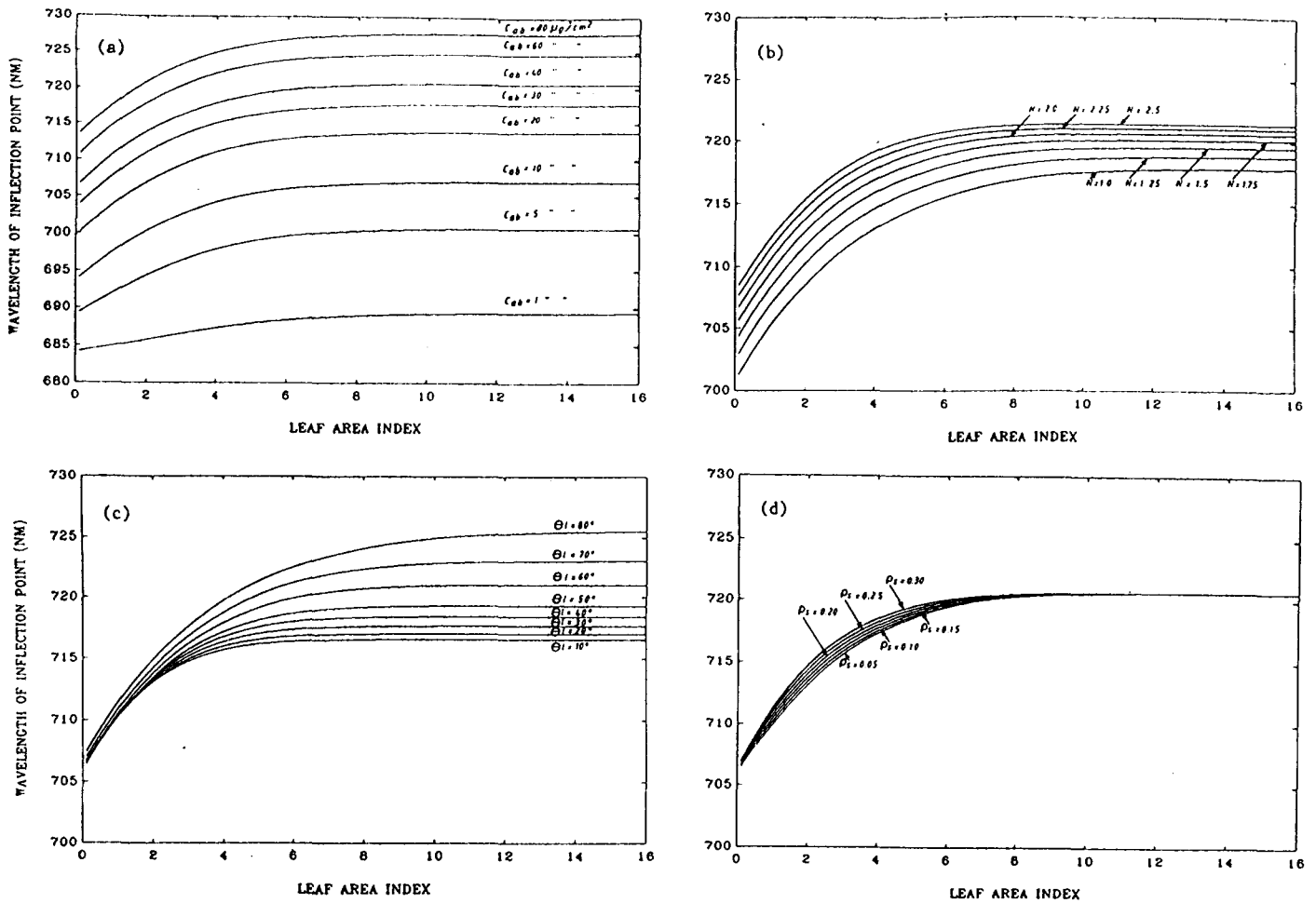
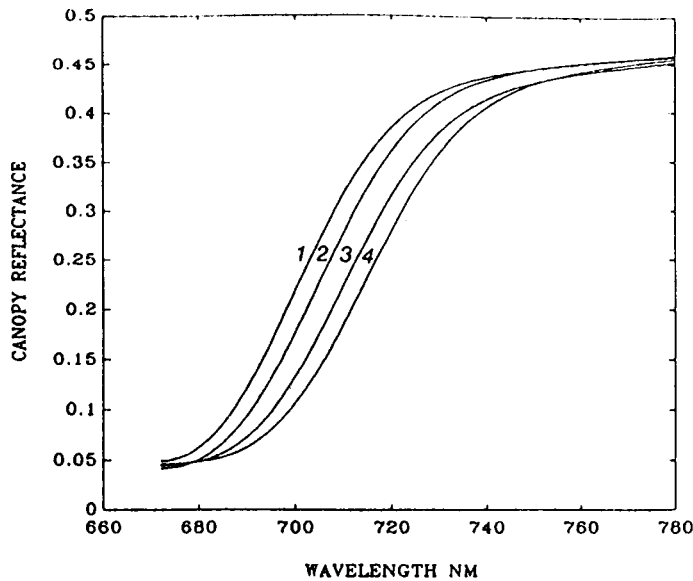


Figure 4. λ_i variations as a function of LAI for vertical viewing.

- (a) : variation with C_{ab} for $X = (C_{ab}, 2, LAI, 0^\circ, 0^\circ, 40^\circ, 58^\circ, 0.15)$
- (b) : variation with N for $X = (40, N, LAI, 0^\circ, 0^\circ, 40^\circ, 58^\circ, 0.15)$
- (c) : variation with θ_1 for $X = (40, 2, LAI, 0^\circ, 0^\circ, 40^\circ, \theta_1, 0.15)$
- (d) : variation with $\rho_s(672)$ for $X = (40, 2, LAI, 0^\circ, 0^\circ, 40^\circ, 58^\circ, \rho_s(672))$

several statistical distributions : a uniform distribution for N ($1 < N < 2.5$), θ_0 ($0^\circ < \theta_0 < 60^\circ$), ψ_0 ($0^\circ < \psi_0 < 180^\circ$), θ_s ($20^\circ < \theta_s < 70^\circ$), θ_1 ($20^\circ < \theta_1 < 80^\circ$) and $\rho_s(672)$ ($0.05 < \rho_s(672) < 0.30$); a lognormal distribution for C_{ab} ($0.1 < C_{ab} < 80 \text{ g}\cdot\text{cm}^{-2}$) and LAI ($0.1 < LAI < 16$). Such a choice is justified by the last analysis revealing a great sensitivity of λ_i for little values of C_{ab} and LAI. The surface corresponding to λ_i as a function of ρ_{672} and ρ_{780} is not as smooth as in the case of a leaf : it shows off some important scattering confirming the nonequivalence between λ_i and ρ_{672} and ρ_{780} and any red-near infrared vegetation index at canopy level. This is in good agreement with experimental data from Baret *et al.* (1987) and Leprieur (1989) who found that the λ_i information content was not strictly the same as the one provided by the Normalized Difference Vegetation Index (NDVI). A given set of red and near infrared reflectance (ρ_{672}, ρ_{780}) may correspond to several values of λ_i (see figure 5). The same conclusions are carried out even if we fix N , θ_0 , ψ_0 , θ_s or $\rho_s(672)$ which have little effect on λ_i and which can be measured or controlled (we let only C_{ab} , LAI and θ_1 vary).



- 1 : $X = (8.8, 2.43, 1.58, 54.5^\circ, 163.3^\circ, 66.6^\circ, 72^\circ, 0.22)$
 2 : $X = (46.5, 2.5, 1.21, 31^\circ, 27.8^\circ, 67^\circ, 45^\circ, 0.25)$
 3 : $X = (35.5, 2.27, 1.02, 48^\circ, 1.8^\circ, 69.3^\circ, 74.6^\circ, 0.18)$
 4 : $X = (17.9, 1.78, 1.9, 37.6^\circ, 106.8^\circ, 60.1^\circ, 44.9^\circ, 0.20)$

Figure 5. Demonstration of the nonequivalence between λ_i versus red and near infrared reflectances (ρ_{672} , ρ_{780}). Spectra 1 to 4 are respectively obtained for the following input variables:

Because any inflection point requires a minimum of 3 data points to be measured, we have added a new single reflectance band in order to test if this extra information significantly contributes to explain the λ_i variance. We have chosen the middle wavelength between the two red edge limits ($710\text{nm} = (780 + 740)/2$). The same set of random input variables is used to compute λ_i , ρ_{672} , ρ_{710} and ρ_{780} . Second order multivariate polynomial fitting of λ_i as a function of $(\rho_{672}, \rho_{710}, \rho_{780})$ explains more than 96% of λ_i variance. The choice of different or additional spectral bands, the use of other types than polynomial fit should explain degree of λ_i with single reflectance wavebands.

From these results, it is concluded as for the leaf level that the λ_i information is very redundant with the information contained in single reflectance wavebands because they depend on the same input variables. However, due to the important number of input variables (at least 8 if one excepts the diffuse/direct incoming radiation ratio), more single wavebands are required to get unambiguous and accurate relationships between spectral shifts and single band reflectance values. Spectral shifts could be then considered as a particular "vegetation index" of interest because of its low sensitivity to disturbing factors such as irradiance conditions or soil brightness and its high sensitivity to canopy characteristics such as chlorophyllian pigments concentration or LAI. But we have still to discuss about the way and the noise associated with the determination of λ_i monitored from space.

3. Spatial measurement of λ_i ; Evaluation of the accuracy and comparison with AVIRIS data.

This section is focussed on problems linked to the use of spectral shifts observed from space and is illustrated by AVIRIS experimental data. We will first and briefly discuss about the disturbing factors such as atmospheric effects and instrumental noise.

3.1. atmospheric effects and instrumental noise.

As it can be demonstrated (Gu, 1988), the signal measured from satellite level (S_{sat}) is related to ground level reflectance (ρ_g) through the linear relationship :

$$S_{sat}(\lambda) = a(\lambda) \cdot \rho_g(\lambda) + b(\lambda) \quad [9]$$

where $a(\lambda)$ and $b(\lambda)$ depend on the atmospheric effects if environmental effects are neglected. Molecular (Rayleigh) and aerosol (Mie) scattering are not very wavelength dependent in the red edge domain at the opposite of gaseous absorption. The 5S model (Tanre *et al.*, 1986) is used to show off the atmospheric gaseous transmittance computed for the AVIRIS spectral bands and for two differing cases (figure 6).

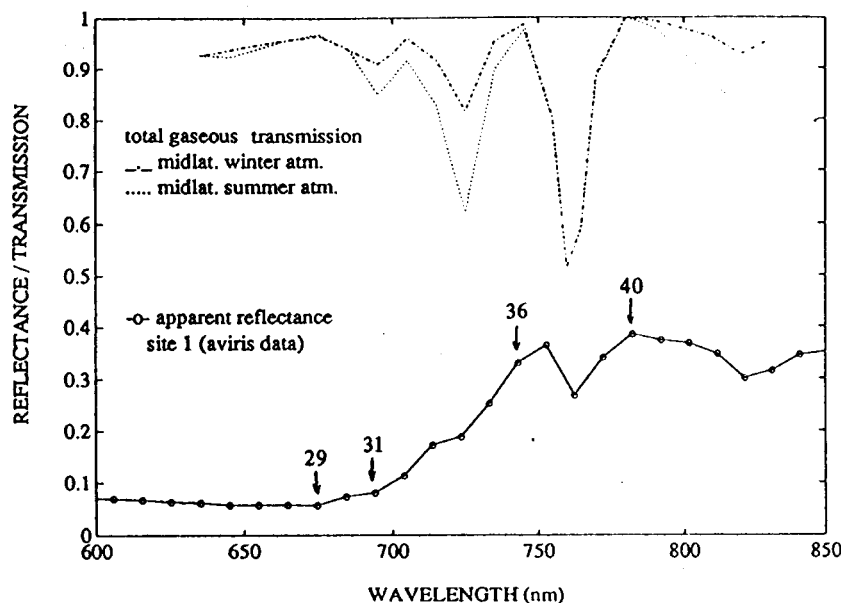


Figure 6. Gaseous transmission computed with 5S model for midlatitude winter and summer atmospheres for the AVIRIS wavebands. The effect on AVIRIS vegetation signal is represented by the bottom curve.

Gaseous absorption creates some strong disturbances on the reflectance spectra collected at satellite level. If channels strongly affected by the gaseous absorption are not used, the atmospheric effects will not affect the determination of λ_i because they just translate the whole spectrum (effect of the b parameter which is no more wavelength sensitive in this case) and transform it by an homothetic factor along the y axis (satellite signal, radiance or reflectance axis). This is one major advantage of this high spectral resolution derived criterion to remove most of the atmospheric effects as discussed previously by Guyot *et al.* (1990).

3.2. Methods of λ_i determination.

A brief review of the literature about the spectral shifts enables us to classify the methods of λ_i determination into 3 main categories :

- * derivation and spectra smoothing : These techniques are used for red edges measured with a lot of narrow spectral bands. It generally corresponds to spectra

performed at leaf or ground level (Horler et al., 1983; Demetriades-Shah and Steven, 1988 among others). Spectra are often smoothed to remove the residual high frequency noise before being derived. This smoothing technique tends to the model inversion technique when the number of parameters to adjust is reduced.

* model inversion techniques : Collins et al. (1983) used Cheybshev decomposition to represent the red edge and compute λ_i . But, as discussed by Gauthier and Neville (1988), this procedure still requires a too large number of spectral data points to be used with spaceborne spectroimagers. Chang and Collins (1983) and Miller et al. (1985) have used a gaussian model to fit the red edge. It requires three parameters and hence a minimum of three independent spectral bands in the red edge (including the minimum reflectance value close to 675 nm and the near infrared shoulder value reached since about 780nm) to be inverted. This procedure is time consuming and may cause problems to use it operationally on large scenes. Because it is also somewhat empirical to choose this particular gaussian model and also because exact inversion of coupled leaf optical properties and canopy reflectance models is delicate due to the number of parameters to adjust, some authors have used a more simplified assessment of λ_i .

* linear model : Because of the quasi linear pattern of the middle of the red edge (from 700 to 740 nm), Gauthier and Neville (1985) have approximated it to a straight line and have characterized the spectral shifts with its intercept at the wavelength axis. Baret et al. (1987) have later shown that the point corresponding to the mid reflectance amplitude of the red edge was a local symmetry centre very close to the true inflection point for green vegetation. Leprieur (1989) applies this definition to AVIRIS data :

$$\lambda_i = \lambda_{31} + (\lambda_{36} - \lambda_{31}) \cdot (\rho_i - \rho_{31}) / (\rho_{36} - \rho_{31}) \quad [10]$$

with $\rho_i = (\rho_{29} + \rho_{40}) / 2$ and the subscripts refer to the AVIRIS channels (29 = 674.4 nm; 31 = 694.0 nm; 36 = 743 nm; 40 = 782.2 nm). We will then use this simple definition of the spectral shift which requires only 4 narrow bands out of the gaseous absorption domain to discuss about the accuracy of its determination from space platforms.

3.3. Evaluation of λ_i accuracy and comparison with AVIRIS data.

The computation of the accuracy is based on the assumption that the errors on the reflectance (or radiance) measurements ($d\rho$) and on the wavelength position ($d\lambda$) of each channel are independent and have the same value ($d\rho$, $d\lambda$) for each of the four channels (Leprieur, 1990). It follows that the maximum error $d\lambda_i$ on λ_i is given by :

$$d\lambda_i = d\lambda + 2 \cdot d\rho \cdot (\lambda_{36} - \lambda_{31}) \cdot (\rho_i - \rho_{31}) / (\rho_{36} - \rho_{31})^2 \quad [11]$$

The error is computed for differing values of LAI for crop with $X = (40, 1.2, \text{LAI}, 0^\circ, 0^\circ, 30^\circ, 58^\circ, 0.15)$. It reveals (figure 7) that $d\lambda_i$ is very important for low leaf area indices and increases drastically with $d\rho$. For larger LAI, the noise level is reduced and mainly depends on $d\lambda$. The computed signal/noise ratios confirm that, even for low errors on λ and ρ ; λ_i estimation should be very noisy compared to its sensitivity to LAI. The same results have been also found for the determination of the chlorophyll

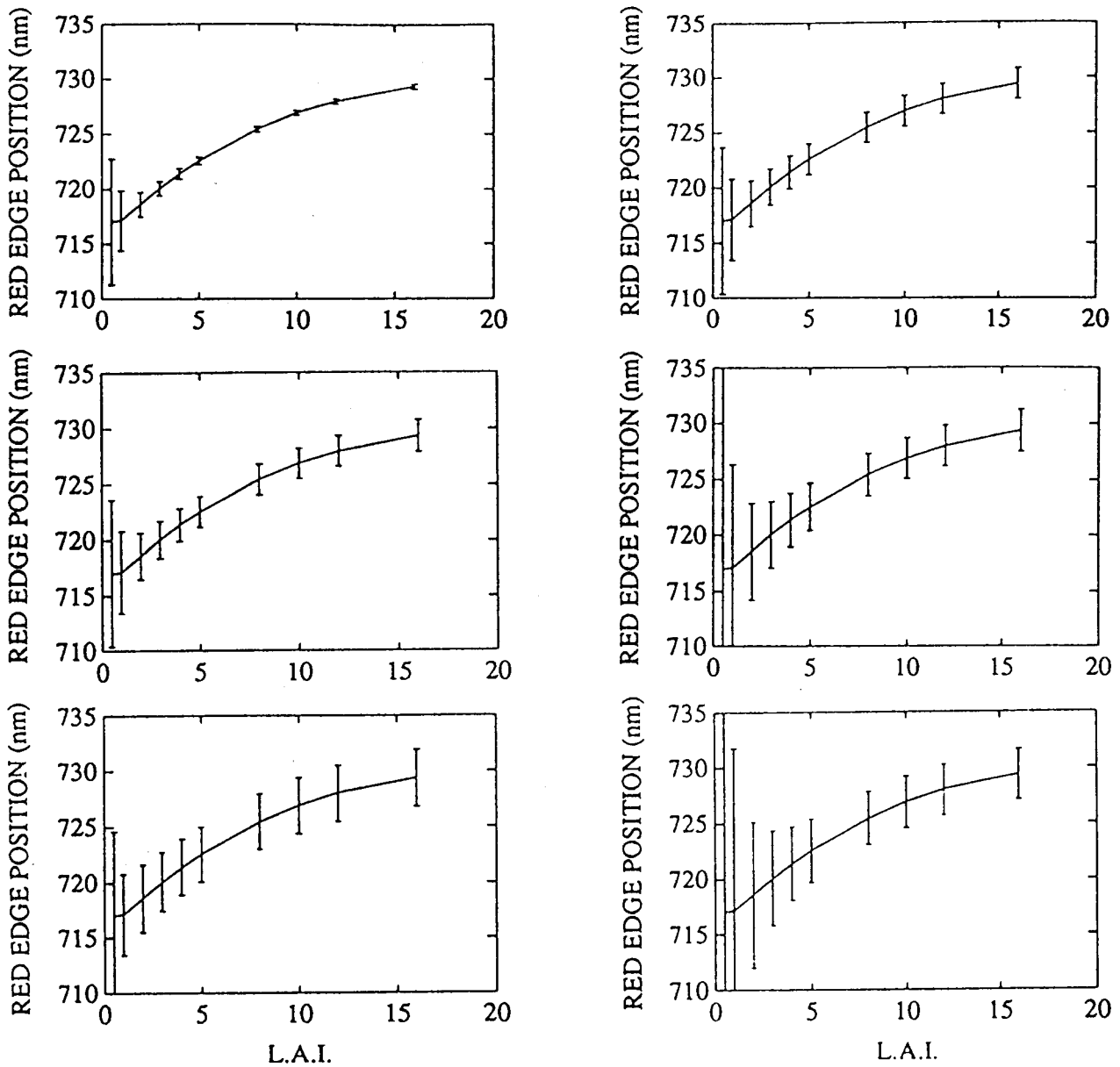


Figure 7. λ_i errors as a function of LAI for differing values of $d\lambda$ and $d\rho$:

- (a): $d\rho = 0.001$; $d\lambda = 0.0$ nm
- (b): $d\rho = 0.001$; $d\lambda = 0.5$ nm
- (c): $d\rho = 0.001$; $d\lambda = 1.0$ nm
- (d): $d\rho = 0.001$; $d\lambda = 0.5$ nm
- (e): $d\rho = 0.003$; $d\lambda = 0.5$ nm
- (f): $d\rho = 0.005$; $d\lambda = 0.5$ nm

content. This evaluation of the error is performed under simplifying assumptions, and should be the maximum one. Because we have no detailed information on the error structure of the spectro-imaging systems, there is no other possibility to get an idea of the noise, except by looking at the discrimination capability on contrasted objects. This has been done on one AVIRIS scene (Moffet field test site in San Francisco Bay). It clearly appears on figure 8 that the λ_i noise is not so important as the one computed.

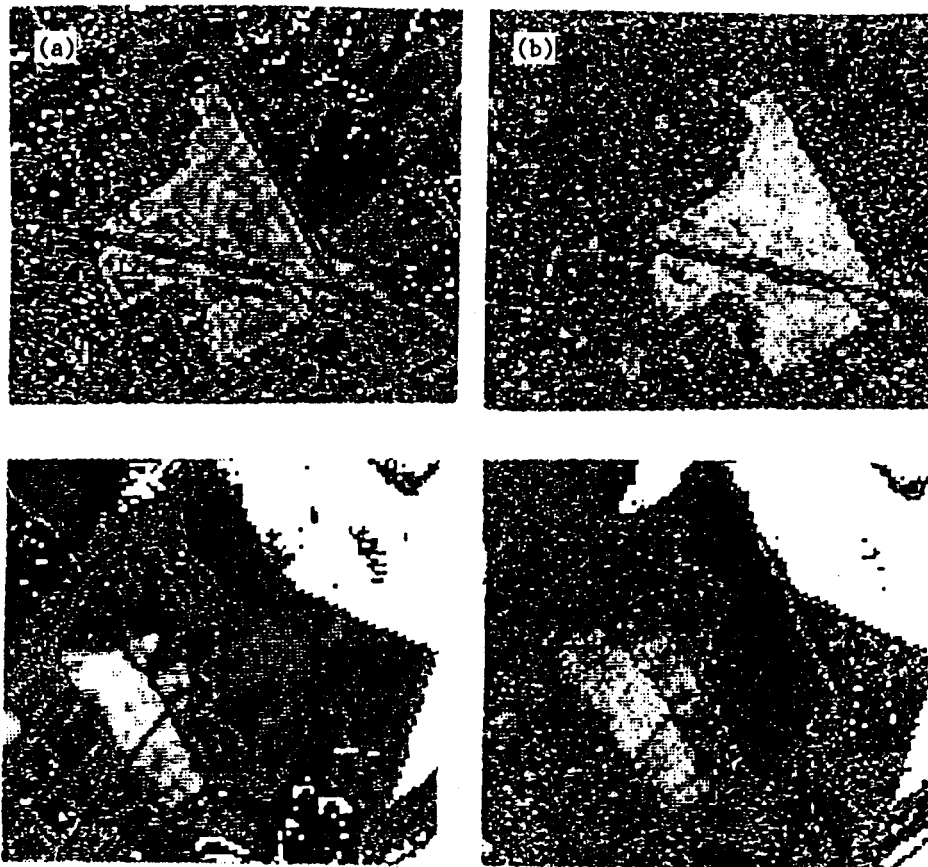


Figure 8. Comparison between NDVI (a) and λ_i (b) observed from AVIRIS on two differing test sites.

Table 1 shows off that for 8 test sites chosen to be representative of the differing vegetation types, the root mean square decreases when green vegetation materials increase as previously expected, but remains around 1.5 nm for a 16 nm maximum range variation of the shifts. It seems to be not too bad as compared to the NDVI which has a corresponding rms close to 0.04 for a maximum range of variation of 0.043.

Site	number pixels	λ_i (nm) mean	λ_i (nm) rms	NDVI mean	NDVI rms
1	203	721.4	1.2	0.74	0.04
2	309	720.1	1.0	0.72	0.03
3	164	719.3	1.0	0.65	0.03
4	118	705.1	1.3	0.55	0.01
5	59	716.4	2.2	0.51	0.05
6	292	715.2	2.4	0.37	0.05
7	146	711.7	2.8	0.32	0.05
8	24	712.3	1.4	0.31	0.06

Table 1. Mean values and rms of λ_i and NDVI computed from 8 test sites.

This apparent contradiction between estimated values of the noise associated to λ_i and the one derived from real AVIRIS data lies in the fact that we have to improve

our knowledge about the instrumental noise structure and refine the error calculation procedure. Nevertheless, this section proves from the experiment that λ_i can be determined with an accuracy equivalent to the one associated to classical vegetation indices as NDVI, except when the vegetation is very scarce. In this case, the low slope of the red edge induces an important error on the determination of the λ_i value.

4. Conclusion.

This brief analysis shows off that the information content of the spectral shifts of the red edge is not different from the one contained in single bands reflectance or vegetation indices. At that stage of the discussion, one could say that spectral shifts are reduced to a particular vegetation index which minimizes external factors such as the irradiance conditions and soil brightness effects. It is very sensitive to the chlorophyll content and the leaf area index, and to a lesser extent, to leaf mesophyll structure and leaf orientation. All of these results obtained through model simulations are in good agreement with the literature. They should be still valid for any "edges" corresponding to a sharp variation of a specific absorption coefficient: One has just to replace the chlorophyll concentration by the corresponding absorbing material content. For example, in the middle infrared, several edges due to water absorption features exist.

When this spectral shift concept is applied at the satellite scale characterized by few wavebands and additional disturbing factors such as instrumental noise and atmospheric effects, the linear model enables getting the shift with only four wavebands. If these wavebands are chosen to be out of the gaseous absorption domain, this spectral shift should be very little dependent upon the atmospheric conditions. This important property is surely one of the main advantages of this spectral shift concept. The theoretical analysis of the noise is actually limited by the bad knowledge about the instrumental error structure. Nevertheless, from real AVIRIS data, it seems that, except for scarce vegetation, the accuracy of the spectral shift determination is close to the one observed for classical vegetation indices.

If High spectral resolution programs are developed until some years, it is certainly to try to improve our knowledge on the target from spaceborne sensors. It seems therefore somewhat restrictive to limit the high spectral resolution capabilities to build empirical indices such as the spectral shifts. The main questions which still remain unsolved are : How many and what wavebands are required to get the full spectral information of canopies ? How can we extract the pertinent characteristics of the vegetation from this spectral information ? And how can we use redundancy between differing channels to remove the atmospheric effects. Researchers have still some time to spend to struggle with these complex problems.

REFERENCES

- Baret F., Champion I., Guyot G., Podaire A., 1987, Monitoring wheat canopies with a high spectral resolution radiometer, *Remote Sens. of Environ.*, 22:367-378
- Campbell G.S., 1986, Extinction coefficients for radiation in plant canopies calculated using ellipsoidal inclination angle distribution, *Agric. & Forest Meteor.*, 36:317-321
- Chang S.H., Collins W., 1983, Confirmation of the airborne biogeophysical mineral exploration technique using laboratory methods, *Econ. Geol.*, Vol. 78, 723-736

- Collins W., 1978, Remote Sensing of crop type and maturity, *Photogram. Eng. and Remote Sens.*, Vol. 44, No. 43, 43-55
- Collins W., Chang S.H., Raines G., Canney F., Ashley R., 1983, Airborne biogeophysical mapping of hidden mineral deposits, *Econ. Geol.*, Vol. 78, 737-749
- Demetriades-Shah T.H., Steven M.D., 1988, High spectral resolution indices for monitoring crop growth and chlorosis, in *Proc. of the 4th Int. Coll. on Spectral Signatures of Objects in Remote Sensing*, Aussois (France), 18-22 January 1988, ESA SP-287, 299-302
- Ferns D.C., Zara S.J., Barber J., 1984, Application of high resolution spectroradiometry to vegetation, *Photogram. Eng. and Remote Sens.*, Vol. 50, No. 12, 1725-1735
- Gates D.M., Keegan H.J., Schleter J.C., Weidner V.R., 1965, Spectral properties of plants, *Appl. Opt.*, Vol. 4, No. 1, 11-20
- Gauthier R.P., Neville R.A., 1985, Narrow-band multispectral imagery of the vegetation red reflectance edge for use in geobotanical remote sensing, in *Proc. 3rd Int. Coll. on Spectral Signatures of Objects in Remote Sensing*, Les Arcs (France), 16-20 Dec., ESA SP-247, 233-236
- Gu Xing-Fa, 1988, Mise en relation des luminances mesurées par SPOT avec les réflectances de surfaces agricoles mesurées au sol, Mémoire de DEA "Méthodes Physiques en Télédétection", INRA-Université Paris VII.
- Guyot G., Baret F., 1990, Potentials and limits of vegetation indices, submitted for publication to *Remote Sens. Environ.*
- Guyot G., Baret F., Jacquemoud S., 1990, Imaging spectroscopy for vegetation studies, in *Imaging Spectroscopy : Fundamentals and Prospective Applications*, F. Toselli and J. Bodechtel ed., Kluwer Academic Publishers (Dordrecht, The Netherlands).
- Horler D.N.H., Dockray M., Barber J., 1983, The red edge of plant leaf reflectance, *Int. J. Remote Sensing*, Vol. 4, No. 2, 273-288
- Jacquemoud S., Baret F., 1990, Modelling leaf optical properties, submitted for publication to *Remote Sens. Environ.*
- Leprieur C.E., 1989, Preliminary evaluation of AVIRIS airborne measurements for vegetation, in *Proc. of the 9th EARSeL Symp.*, Espoo (Finland), 27 June - 1 July, 6 p
- Leprieur C.E., 1990, Comparaison des ordres de grandeur des mesures et des erreurs théoriques associées en haute résolution spectrale (domaine visible et proche infrarouge), LERTS-CNES unpublished works
- Miller J.R., Hare E.W., Neville R.A., Gauthier R.P., McColl D., Till S.M., 1985, Correlation of metal concentration with anomalies in narrow band multispectral imagery of the vegetation red reflectance edge, in *Proc. of the Int. Symp. on Remote Sensing of Environ.*, 4th Thematic Conference, Remote Sensing for Exploration Geology, San Fransisco, April 1-4, 143-153

- Richardson A.J., Wiegand C.L., 1977, Distinguishing vegetation from soil-background information, *Photogram. Eng. and Remote Sens.*, 43:1541-1542
- Rock B.N., Hoshizaki T., Miller J.R., 1988a, Comparison of *in situ* and airborne spectral measurements of the blue shift associated with forest decline, *Remote Sens. Environ.*, 24:109-127
- Rock B.N., Elvidge C.D., Defeo N.J., 1988b, Assessment of AVIRIS data from vegetated sites in the Owens Valley, California, In *Proc. of the Airborne Visible/Infrared Imaging Spectrometer (AVIRIS) Performance Evaluation*, Workshop June 6,7 and 8 1988, Gregg Vane Editor, NASA-JPL publication 88-38, 88-96
- Tanré D., Deroo C., Dahaut P., Herman M., Morcrette J.J., Perbos J., Deschamps P.Y., 1986, Effets atmosphériques en télédétection. Logiciel de simulation du signal satellitaire dans le spectre solaire, in *Proc. 3rd Int. Coll. on Spectral Signatures of Objects in Remote Sensing*, Les Arcs (France), 16-20 Dec., ESA SP-247, 315-319.
- Vanderbilt V.C., Ustin S.L., Clark J., 1988, Canopy geometry changes due to wind cause red edge spectral shift, in *Proc. of IGARSS'88 Symp.*, Edinburgh (Scotland), 13-16 Sept., ESA SP-284, 835
- Verhoef W., 1984, Light scattering by leaf layers with application to canopy reflectance modeling : the SAIL model, *Remote Sens. Environ.*, 16:125-141
- Verhoef W., 1985, Earth Observation modeling based on layer scattering matrices, *Remote Sens. Environ.*, 17:165-178
- Wang Y.P., Jarvis P.G., 1988, Mean leaf angles for the ellipsoidal inclination angle distribution, *Agric. & Forest Meteor.*, 43:319-321